CHAPTER 3

EXPERIMENTAL SETUP

3.1 ZEUS Experiment

ZEUS experiment began its first operation in 1992. The experiment mainly consists of two main giant equipments, the HERA collider and ZEUS detector, which used to accelerate and detect particle from electron and proton collision respectively. Generally, the experiment is dedicated to observe the particles productions at high energy physics events of lepton-hadron collision as well as observing the particle characters.

3.2 HERA Collider

The HERA ring is located at DESY, Hamburg. It was constructed 30m underground deep and 6.3km long in circumference. It was the first e-p collider designed to accelerate the electron and proton from opposite direction before collisions take place inside the detection system or detector.

The electron and proton beampipe are placed on top of each other along the HERA ring. The electron beampipe consist of normal conducting dipole-magnets with 0.3T and super-conducting cavities to accelerate electron beam up to 27.5 GeV. Meanwhile the proton beampipe has the feature of 4.7 T dipole-magnets conductivity and can be accelerated up to 920 GeV in HERA ring. The squared centre-of-mass energy for e-p collision, $\sqrt{s}$ was measured to be 300 until year 1997 and then changed to 318 after the e-p acceleration energy upgrading until the operation stopped in 2007. HERA was built with four interaction points where detectors are placed. The H1 and ZEUS detectors are designed for the e-p interaction. Meanwhile HERMES is used for research on the spin structure which only utilizes an electron beam. The forth detector, HERA-B investigates CP violation in the $B^0\overline{B}^0$-system by using the proton beam together with a fixed wire target. Each of these experiments have contributed significantly to for particle physics research.

The proton and electron originate at different starting points. Protons were firstly stripped off from negative hydrogen ions (H^-) in LINAC III and injected with energies of 50 MeV. Then the proton was transferred to the DESY III ring and injected to 7 GeV before moving to the bigger ring of PETRA with a higher energy injection of 40 GeV. Lastly, the proton was transferred to the biggest ring, HERA with the highest energy of 920 GeV. Meanwhile, electrons started at LINAC II with energies of 450 MeV before moving to DESY II ring with higher energy injection of 7.5 GeV. Moving on to PETRA, the energy of the electrons were subsequently injected up to 14 GeV and ready to accelerate at highest energies of 27.5 GeV in HERA afterwards. HERA could be filled with a maximum of 210 bunches of leptons and protons at a time where each of them were separated by 96 ns [13-16].

Figure 3.1: An aerial view of HERA showing the location of the accelerators.

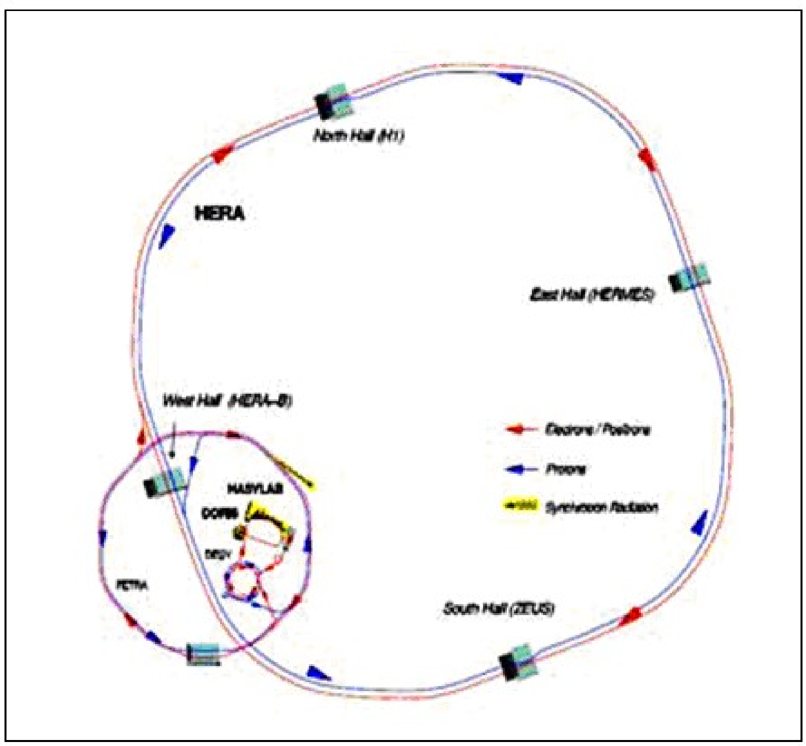

Figure 3.2: This diagram shows the direction of the electron and proton injection flows. The red arrow represents the electron and the blue arrows represent the proton.

3.3 ZEUS Detector

The ZEUS detector [17] was located 30 m underground at south direction of HERA. The weight was about 3500 tons and was 12 meters in height. It was a multipurpose detector with a solid angle coverage of 99.6% and implement the right-handed schematic system. The centre of the system was at the nominal interaction point (IP), the z-axis was pointing to the forward direction (proton direction), the x-axis was pointing towards the centre of HERA and the y-axis was pointing upward.

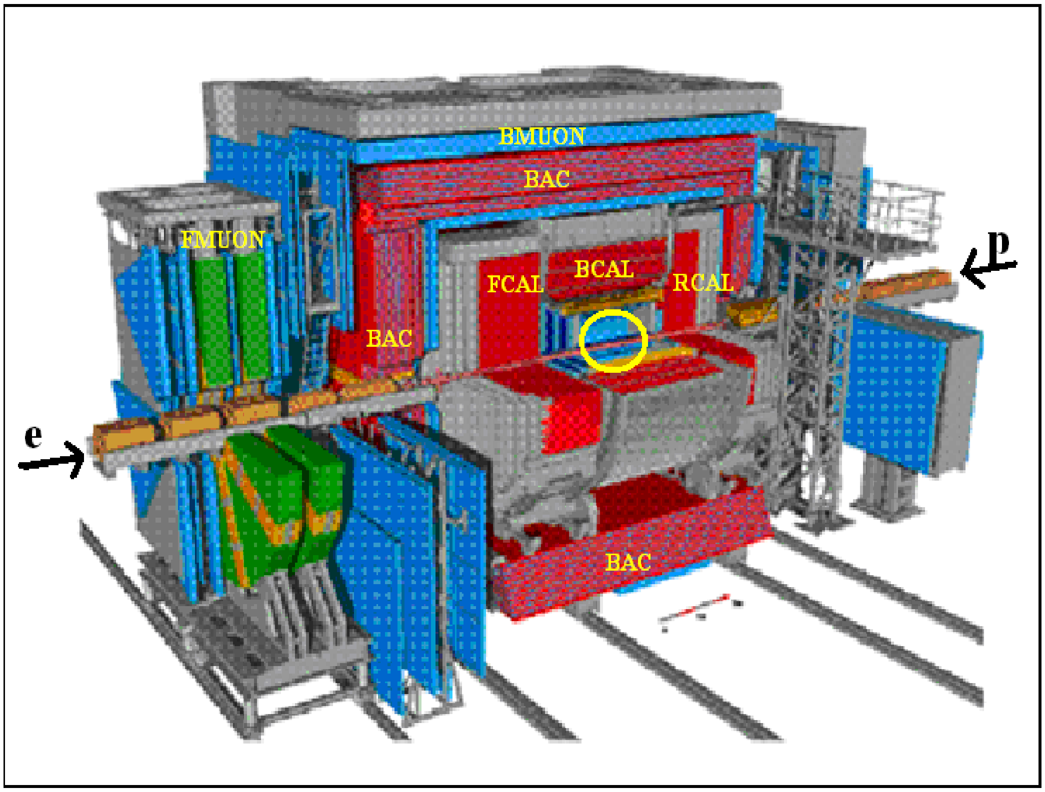

Figure 3.3: The picture shows a 3-dimentional view of a ZEUS detector, its main components and the electron proton directions. The circled area indicates the interaction point of the electron proton collision.

The polar angle, θ and the azimuthal angle, ϕ were measured relative to the *z* and *x* axes respectively. Usually, θ angle was described in pseudorapidity form, $\eta = -\ln\left(\tan\frac{\theta}{2}\right)$. There was an obvious symmetry imbalance between the forward and rear side of the detector. The forward side was longer than the rear part. This was because of the huge different in momentum values of proton and electron, which giving a bigger particle boosting towards the forward direction.

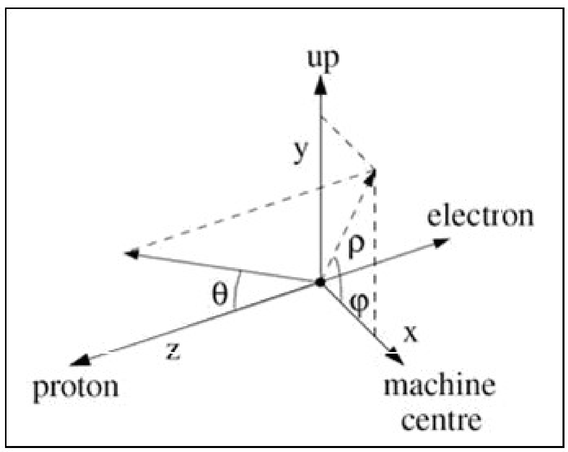

Figure 3.4: The picture shows the coordinate system of the ZEUS detector.

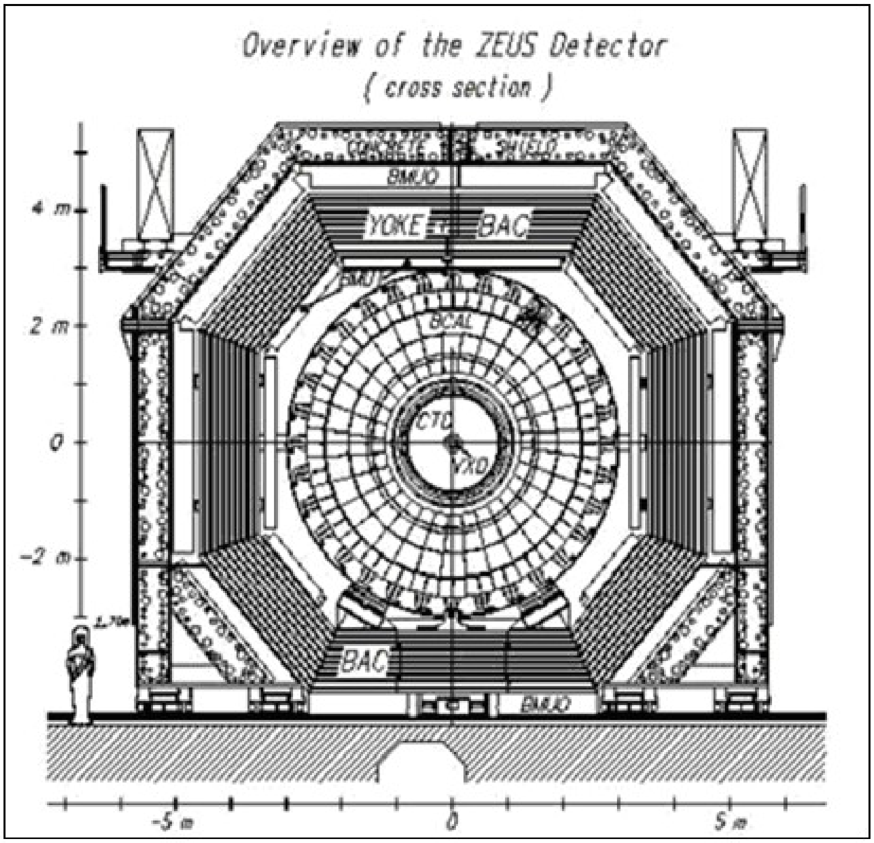

Figure 3.5 : Cross section of the ZEUS detector in x-y plane.

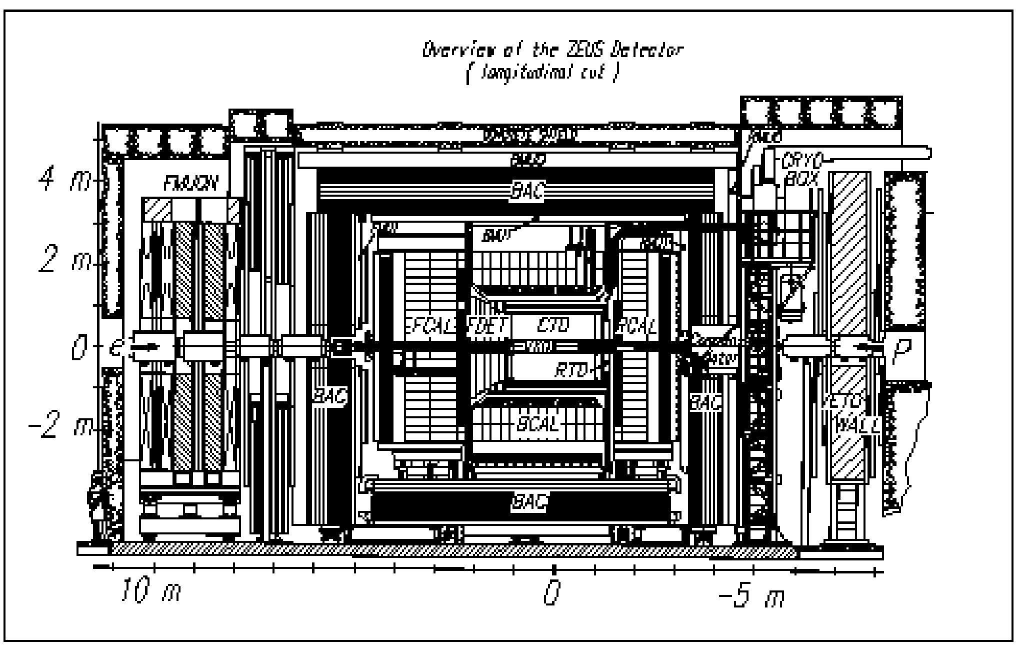

Figure 3.6: Cross section of the ZEUS detector in z-y plane.

3.4 Muon Detection System

The muon is recognized as a minimum ionizing particle (MIP) which leaves tracks signature in many different subdetectors such as tracking, calorimeter and the external muon detection systems. It has a high penetration power allowing it to go through almost all detector layers. The range of muons in iron is about 1 m/GeV. Basically in ZEUS detector, there are three main components of muon detectors; the forward muon detector (FMUON), the barrel muon detector (BMUON) and the real muon detector (RMUON). Figure 3.7 and 3.8 shows the picture of the muon detector components in ZEUS detector.

The muon finder for the ZEUS detector is called the GMUON. It is a combination of all muon finders available at ZEUS. It establishes links between finders and assigns a global muon quality. The GMUON is implemented in the context of ORANGE analysis environment. The cross reference to the other ORANGE information (tracks, jets, MC true and etc.) also provided. Traditionally, we need a specific selection of one or two such algorithm which was available as private code in each muon analysis. Obviously, this process is a tedious way of doing the analysis. To have more efficiency in muon analysis, the GMUON [43] finder has been created. The purpose of GMUON is to combine the most important information from different finders into a common format without private code. It is also able to combine information of the same muon from different finders into single entries as much as possible. Users also have freedom to select their finders and cuts as the GMUON will provide cross reference to the individual finders. GMUON also provide a global muon quality flag which allow the average user to preselect muons without need to know all the details about finders.

Muon can be detected in different ways and signature. It can be identified by the characteristic of its charge penetration in the subdetector. The tracks of this penetration can be seen in the inner tracking detector such as the Micro Vertex Detector (MVD), Central Tracking Detector (CTD) [18-20], and so on. These tracks are bent in the ZEUS solenoid field and their curvature can be used to determine the muon momentum. The muons that are famous in physics are produced either directly at the primary vertex, or in semileptonic heavy flavor decays very close to the primary vertex. Muons, as a MIP particle, lose a well defined amount of energy in the calorimeter along their trajectory. This energy loss is almost independent of muon momentum. The pattern of this energy loss is significantly important to identify muons which do not overlap with any other particles and well isolated. Since the other particles will lose all their energy in the calorimeters, therefore the separation power for muon detection using the MIPs increases with the increasing muon momentum. However, if the muon is a non-isolated particle which overlaps with other particles, MIPs cannot be used in the detection.

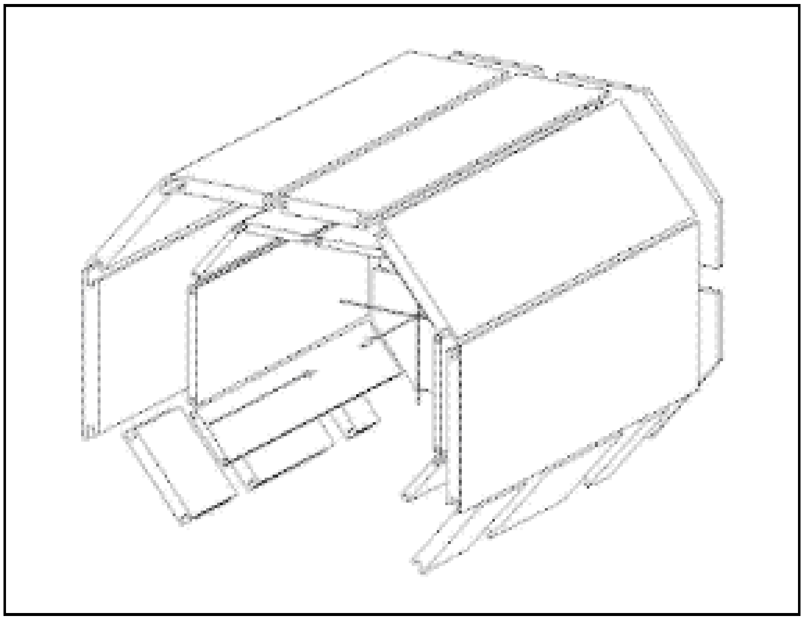

Figure 3.7 : 3D structure of BRMUON

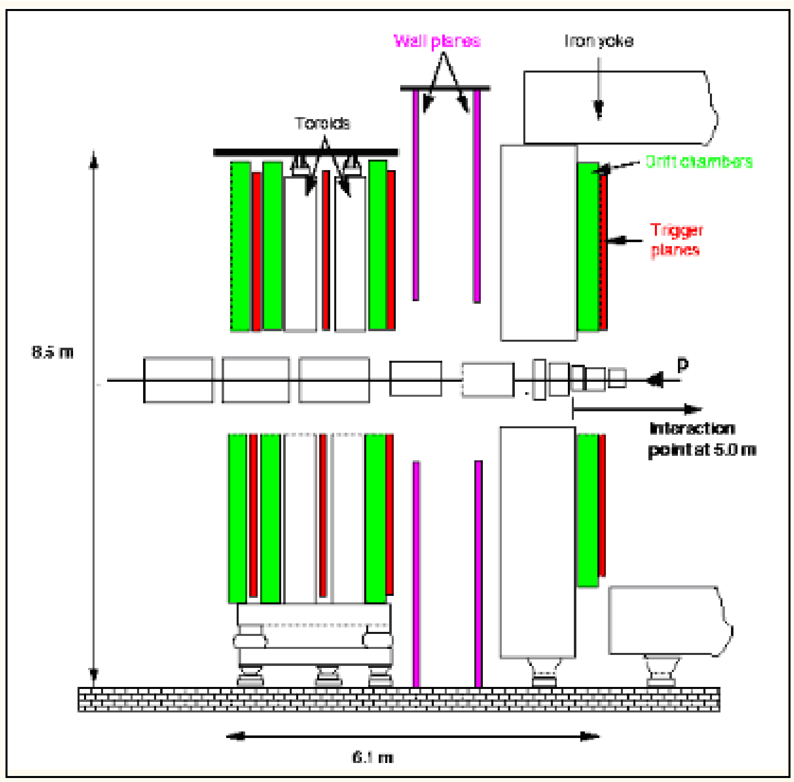

Figure 3.8 : Cross section of FMUON

3.5 Central Tracking Detector (CTD)

The CTD [18-20] is a cylindrical wire drift chamber with a magnetic field of 1.43 T which is provided by a thin superconducting solenoid. The CTD is used to measure the directions and momenta of the charged particle and estimate the energy loss dE/dx to provide information for particle identification. It has 72 cylindrical drift chamber layers of sense wires, organized in 9 superlayers covering the polar angle 15° to 164°. Each superlayer consist of 8 sense wires with associated field wires, called a cell. The drift cells of all superlayers are similar. There are a total of 4608 sense wires and 19584 field wires in the CTD. The inner radius of the chamber is 79.4cm, and its active region covered the longitudinal distance of -100 cm < z < 104 cm. The sense wires were 30 μm thick while the field wires have different diameters. Each superlayer was numbered accordingly from the inner layer to the outer layer. The odd layer consists of tools which were used to determine the z-position by using the time different between the arrival times of the signal from the opposite end of the CTD. The CTD was filled with a mixture of argon (Ar), carbon dioxide (CO_2) and ethane (C_2H_6) in the ratio 85 : 5 : 1. A charged particle crossing the CTD produced ionization of the gas in the chamber. The electrons from the ionization drifted towards the positive sense wires whereas the positively charged ions drifted toward the negative field wires. The CTD hit resolution of HERA I was 200 μm in the $r-\phi$ plane and 2 mm in the z coordinate. The resolution on p_T for tracks fitted to the interaction vertex and passing at least three CTD superlayers and with p_T > 150 MeV, is given by:

$$\frac{\sigma(p_T)}{p_T} = 0.0058 \cdot p_T \oplus 0.0065 \oplus \frac{0.0014}{p_T}$$

where p_T is given in GeV and the symbol $\oplus$ indicates the quadratic sum. Meanwhile for HERA II, the new additional tracking equipment has been installed to improve the tracking resolution which is called the micro vertex detector (MVD).

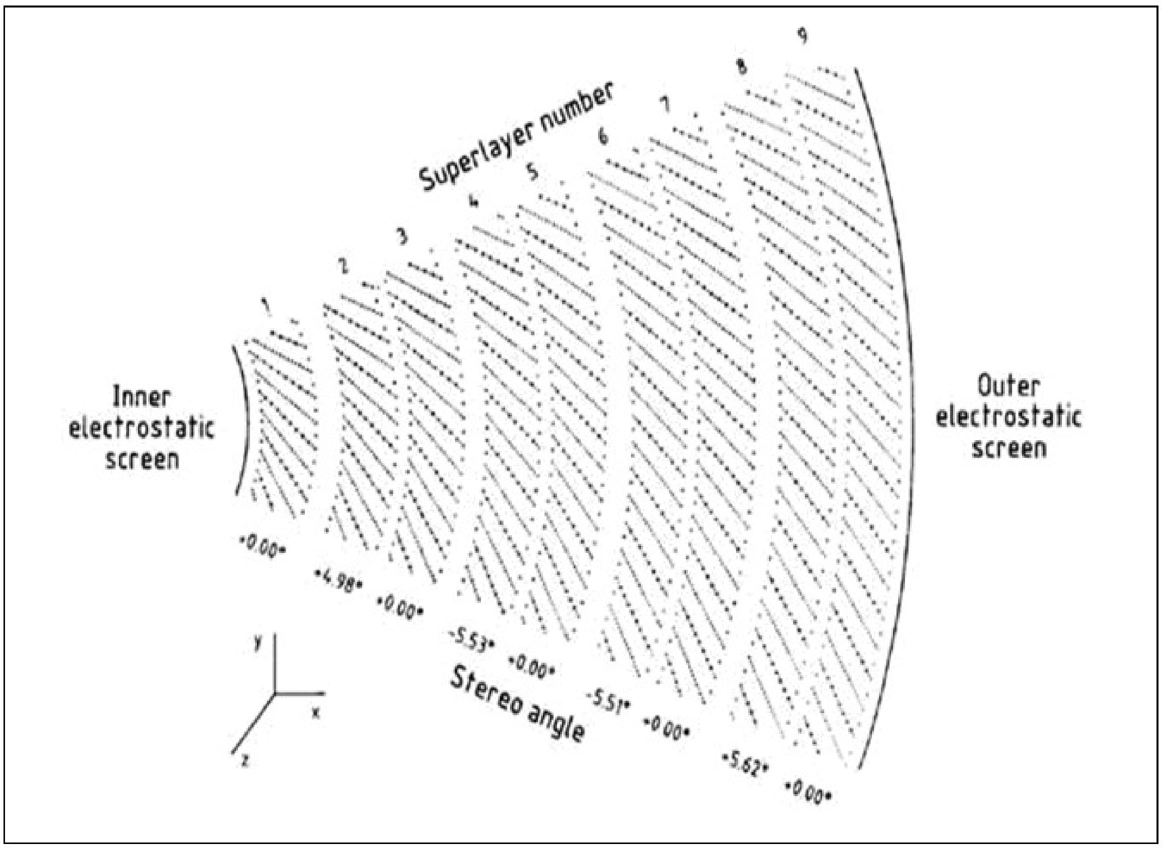

Figure 3.9: Layout of a CTD octant. The superlayers are numbered and the stereo angles of their sense wires are shown.

3.6 Micro Vertex Detector (MVD)

The silicon-strip micro vertex detector (MVD) [21] was installed in 2001. It aimed at a significant improvement of the tracking capabilities to permit the reconstruction of impact parameters and secondary vertices. Figure 3.10 displays the layout of the MVD, which is split into a barrel and a forward region. The sensitive areas are called ladders and contain two layers of orthogonally oriented silicon strips.

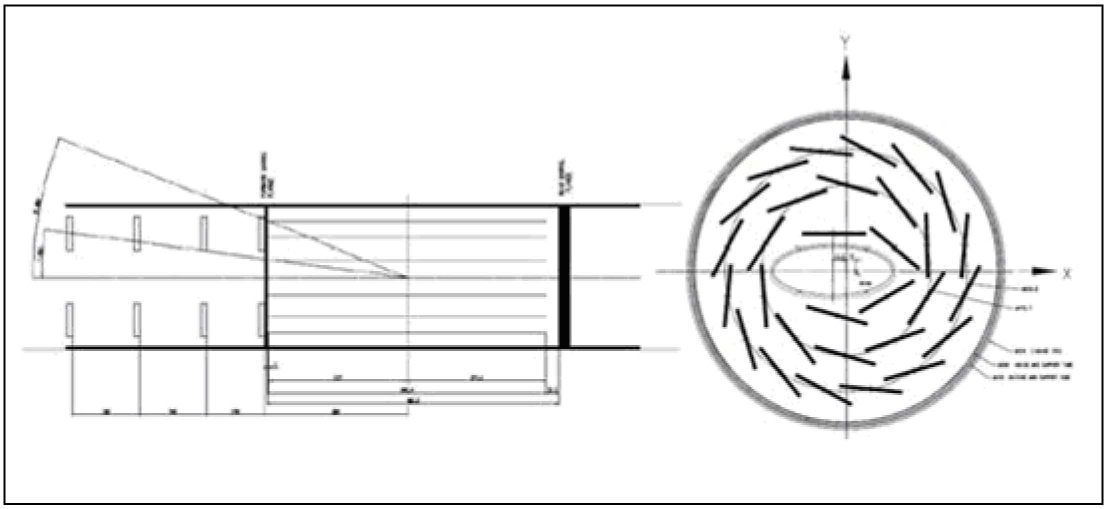

Figure 3.10: Cross sections of the MVD along the beam pipe (left) and in the X-Y plane (right).

The MVD measured the charge-deposit on its strips. In combination with the known geometry of the detector and the orientation of the tracks this was used to measure the ionization rate. It is possible to use the MVD for particle identification in a similar way as the CTD. As one can observe in Fig. 3.10 a typical track passes 3 ladders, i.e. at most 6 silicon strips. This number is small compared to the number of hits for a typical track in the CTD. Performance comparison of the tracking used for HERA I data samples (CTDonly) to the tracking used for the HERA II data (MVD-CTD: 2003-2007, and MVD-CTD-STT: 2003-2007 excluding 2005) is not a trivial task.. The track transverse momentum resolution improved by ≈ 50%. The vertex position in x-y plane improved changing from ~ 0.1 cm (HERA I) to better than 0.01 cm (HERA II). The z-coordinate of the vertex position also improved due to a few extra hits located closer to the interaction point, however having no consequences for the analysis. The cuts defining the vertex position in *x*, *y*, *z* coordinates were conservative remaining identical to the ones used in the analyses of HERA I data samples only.

3.7 Forward and Rear Tracking Detectors (FTD, RTD)

The FTD [22] measured the tracks of charged particles in planar drift chambers located at the ends of the central tracking detector in forward (proton) and rear (electron) directions.

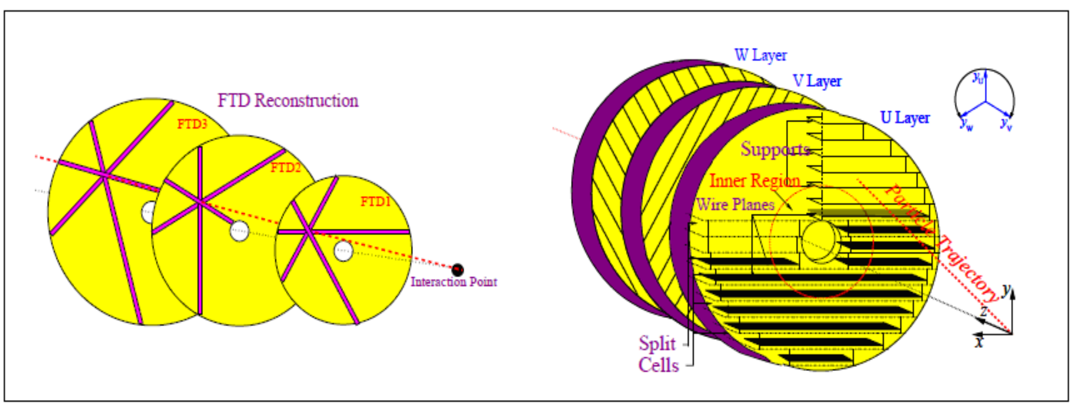

Figure 3.11: The Layout of the FTD drift chambers in (left) overall view and (right) view of the 3 layers inside of one of the chambers.

A charged particle passed in the FTD through 3 chambers (RTD - 1 chamber). Each chamber contained 3 layers with a total of 18 wire planes. The layers consisted of drift cells which were rotated by 60 degrees with respect to each other. The FTD cells are rectangular with six signal wires strung perpendicular to the beam axis.

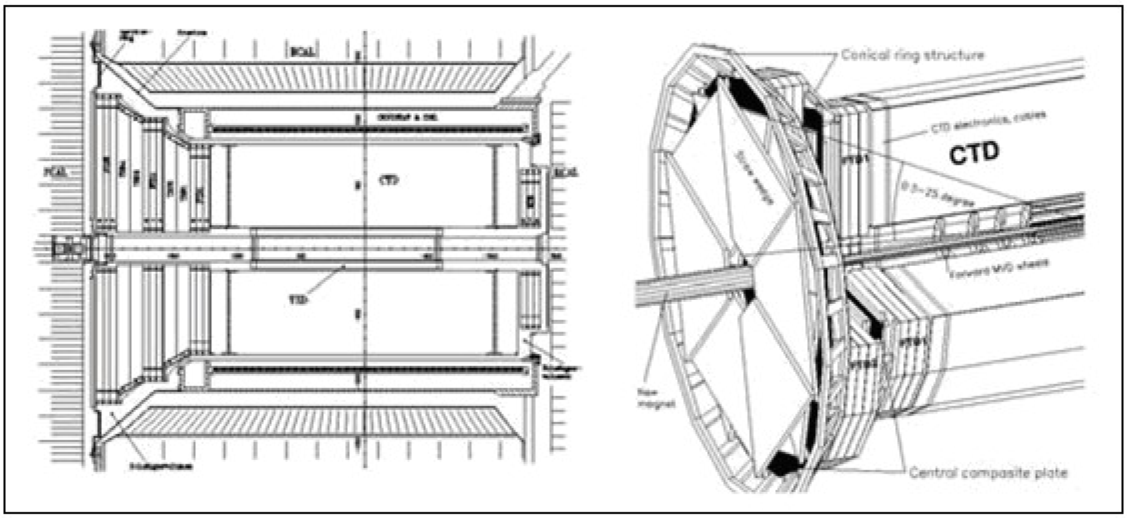

Figure 3.12: (left) a view of the tracking detectors, in the forward area the four tracking detectors planes are shown, which were replaced with two straw-tube tracker (STT) [23] wheels, (right) the angular coverage of the STT compared to the CTD and forward MVD wheels.

3.8 Uranium Calorimeter (CAL)

The ZEUS calorimeter (CAL) [24-27] is a high-resolution compensating calorimeter. It completely surrounds the tracking devices and the solenoid, and covers 99.7% of the 4π solid angle. It consists of 3.3 mm thick depleted uranium plates (98.1% U^{238}, 1.7% Nb, 0.2% U^{235}) as absorber alternated with 2.6 mm thick organic scintillators (SCSN-38 polystyrene) as active material. The thickness of the absorber and of the active material have been chosen in order to have the same response for an electron or a hadron of the same energy passing through the detector (e/h = 1.00±0.05). This mechanism is called compensation, and allows achieving good resolution in the determination of both the electromagnetic and the hadronic energy.

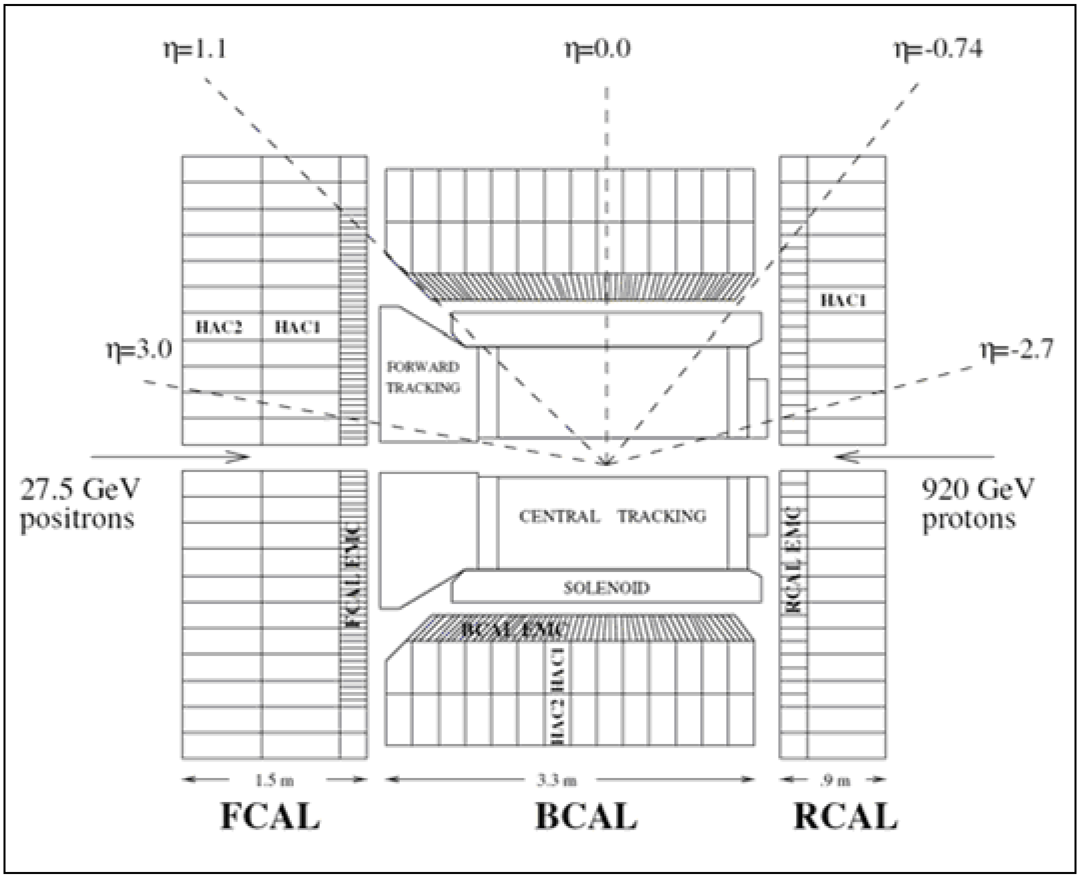

Figure 3.13: Cross section of the ZEUS CAL in the y-z plane.

The achieved hadronic energy resolution is

$$\frac{\Delta E}{E} = \frac{35\%}{\sqrt{E}} \oplus 1\% \tag{23}$$

while the electromagnetic resolution is

$$\frac{\Delta E}{E} = \frac{18\%}{\sqrt{E}} \oplus 2\% \qquad (24)$$

where ΔE is the particle energy, measured in GeV. The CAL is divided into three parts: the forward (FCAL), barrel (BCAL) and rear (RCAL) calorimeters.

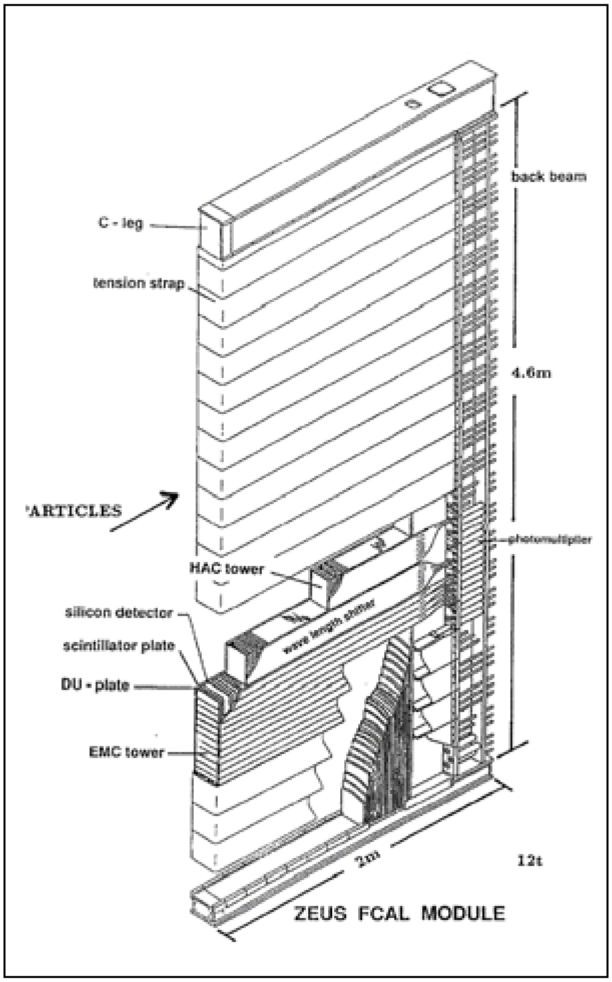

Figure 3.14: View of an FCAL module. The towers containing the EMC and HAC sections are shown.

The three parts are of different thickness, the thickest one being the FCAL (~ 7λ), then the BCAL (~ 5λ) and finally the RCAL (~ 4λ), where λ is the track length. Each part of the calorimeter is divided into modules, and each module is divided into one electromagnetic (EMC) and two (one in RCAL) hadronic (HAC) sections. These sections are made up of cells, whose sizes depend on the type (EMC or HAC) and position (in FCAL, BCAL or RCAL) of the cell. The FCAL consists of one EMC (first 25 uranium-scintillator layers) and two HAC (remaining 160 uranium-scintillator layers) sections. The electromagnetic section has a depth of ≈ 26 X_0, while each hadronic section is 3.1 λ deep.

The EMC and HAC cells are superimposed to form a rectangular module, one of which is shown in Fig. 3.14 and 23 of these modules make up the FCAL. The BCAL consists of one EMC and two HAC sections, the EMC being made of the first 21 uranium-scintillator layers, the two HACs of the remaining 98 layers. The resulting depth is 21 X_0 for the electromagnetic section, and 2 λ for each hadronic section. The cells are organised in 32 wedge-shaped modules, each covering 11.25^o in azimuth. The RCAL is made up of 23 modules similar to those in the FCAL, but it consists of one EMC and only one HAC section. Therefore its depth is 26 X_0 for the EMC part and 3.1 λ for the HAC part. The light produced in the scintillators is read by 2 mm thick wavelength shifter (WLS) bars at both sides of the module, and brought to one of the 11386 photomultiplier tubes (PMT) where it is converted into an electrical signal. This information is used for energy and time measurements. The CAL provides accurate timing information, with a resolution of the order of 1 ns for tracks with an energy deposit greater than 1 GeV. This information can be used to determine the timing of the particle with respect to the bunch-crossing time, and it is very useful for trigger purposes in order to reject background events. The stability of the PMTs and of the electronics is monitored with lasers and charge pulses. In addition, the small signal coming from the natural radioactivity of the depleted uranium gives a very stable signal, also used for the calibration. The achieved accuracy is better than 1%.

3.9 Monte Carlo Generator for Vector Meson

The simulation of the vector meson production and decay is implemented in the DIFFVM 2.0 [28] software package. The software program implements Regge phenomenology and the Vector Dominance Model (see Chapter 2.3.2) with a set of parameters, which can be set via control cards. S-Channel Helicity Conservation (SCHC) is assumed in the generation of the angular distribution of the decay products. The program is primarily used to generate samples of elastic production of the vector mesons. Processes with dissociation of the proton can be generated as well. For the generation of the proton remnant spectrum DIFFVM uses a parametrisation of the experimental data of the mass spectra of excited states of hadrons. This spectrum consists of some resonances-like structures superimposed on the diffraction dissociation continuum. The inclusive cross section for diffractive processes, at fixed t, can be parametrised as follows:

$$\frac{d\sigma}{dM_Y^2} \sim \frac{f(M_Y^2)}{M_Y^{2(1+\epsilon)}} \tag{25}$$

where $f(M_Y^2)$ is a function of the diffractive mass at the proton vertex accounting for the low mass behaviour, including the resonance states.

DIFFVM uses the following parametrisation for this function:

- in the continuum region ($M_Y^2 \geq 3.6$ GeV^2), $f(M_Y^2) = 1$; this reproduces the behaviour ~ $\frac{1}{M_Y^{2(1+\epsilon)}}$ of diffractive dissociation,
- in the "resonance region" ($M_Y^2 < 3.6$ GeV 2), $f(M_Y^2)$ is the result of a fit of the measured differential cross section, at fixed t, for proton diffractive dissociation on deuterium $pD \to YD$;

The continuum state may dissociate into a quark-diquark system (simulated via JETSET) or decay isotropically. The t-distribution b parameter is set:

$$b(W, M_Y) = b(W_0, M_0) + 4\alpha'_p \left(\ln \frac{W}{W_0} - \ln \frac{M_Y}{M_0} \right) \tag{26}$$

and is assumed to hold at all values of Q2.

The W and Q2 dependence of the cross section is given by:

$$\sigma^{\gamma^* p}(Q^2, W) \sim \frac{W^\delta}{(Q^2 + M_V^2)^n} \tag{27}$$

where n ≈ 2.5 is an empirical parameter, $\delta = 4(\alpha\ p\ (0) - 1)$ and M_V mass of the vector meson.

The ratio of the cross sections of the photons with transverse and longitudinal polarisation is given by:

$$R(Q^2) = \frac{\xi \frac{Q^2}{\Lambda^2}}{1 + \chi \xi \frac{Q^2}{\Lambda^2}} \tag{28}$$

where Λ, χ, ξ are free parameters. The recommended values are $\Lambda = M_V$, $\chi = 0.66$, $\xi = 0.33$.